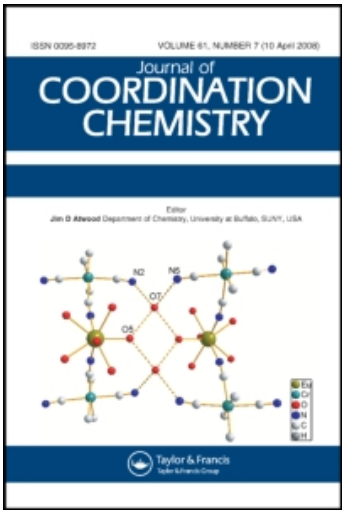

Journal of Coordination Chemistry
Publication details, including instructions for authors and subscription information:
http://www.informaworld.com/smpp/title~content=t713455674

Asymmetric dibenzoylated monobenzotetraazacyclo[15]annulenenickel(II) complexes

E. H. Kim[a]; D. I. Kim[a]; I. J. Park[a]; Z. U. Bae[a]; J. C. Byun[b]; H. G. Na[c]; Y. C. Park[a]
[a] Department of Chemistry, Kyungpook National University, Daegu 702-701, Korea [b] Department of Chemistry, Cheju National University, Cheju 690-756, Korea [c] Department of Chemistry, Daejin University, Pochon 487-800, Korea

To cite this Article Kim, E. H. , Kim, D. I. , Park, I. J. , Bae, Z. U. , Byun, J. C. , Na, H. G. and Park, Y. C.(2007) 'Asymmetric dibenzoylated monobenzotetraazacyclo[15]annulenenickel(II) complexes', Journal of Coordination Chemistry, 60: 4, 411 — 421
To link to this Article: DOI: 10.1080/00958970600794875
URL: http://dx.doi.org/10.1080/00958970600794875

Journal of Coordination Chemistry
Vol. 60, No. 4, 20 February 2007, 411–421

Asymmetric dibenzoylated monobenzotetraazacyclo[15]annulenenickel(II) complexes

E. H. KIM†, D. I. KIM†, I. J. PARK†, Z. U. BAE†,
J. C. BYUN‡, H. G. NA§ and Y. C. PARK*†

†Department of Chemistry, Kyungpook National University, Daegu 702-701, Korea
‡Department of Chemistry, Cheju National University, Cheju 690-756, Korea
§Department of Chemistry, Daejin University, Pochon 487-800, Korea

(*Received in final form 4 March 2006*)

The 15-membered asymmetric complexes, 3,11-di(*p*-Xbenzoyl)-2,4,10,12-tetramethyl-1,5,9, 13-monobenzotetraazacyclo[15]annulenenickel(II), X = CH_3, H, Cl, NO_2 and OCH_3, were synthesized and characterized. IR spectra of the benzoylated complexes showed an intense C=O stretching mode in the range 1630–1640 cm^{-1}. Hammett plots of λ_{max}^{-1} of $\pi \rightarrow \pi^*$ and LMCT were linear with slopes of +0.379 and +0.339, respectively. ^{1}H NMR signals of methyl groups showed shielding effects due to magnetic anisotropy of benzoyl groups, while other proton signals exhibited deshielding effects. ^{13}C NMR spectra were consistent with ^{1}H NMR. Voltammograms of complexes showed two irreversible oxidation peaks due to the ligands in the ranges +0.35 to +0.44 V and +0.74 to +0.86 V, respectively. A reduction wave involving nickel(II) was found in the range −2.50 to −2.70 V, depending on substituents on the benzoyl group. Hammett plots of the first and second oxidation potentials had linear slopes of +0.071 and +0.104, respectively. The structures of 2,4,10,12-tetramethyl-1,5,9, 13-monobenzotetraazacyclo[15]annulenenickel(II) (monoclinic, $C2/c$, $a = 22.883(6)$, $b = 10.358(3)$, $c = 14.755(4)$ Å, $\beta = 102.704(4)^\circ$, $Z = 8$, $R1$ $[I > 2\sigma(I)] = 0.0295$, wR_2 $[I > 2\sigma(I)] = 0.0744$) and 3,11-di(*p*-methylbenzoyl)-2,4,10,12-tetramethyl-1,5,9,13-monobenzotetraazacyclo[15]annulenenickel(II) (orthorhombic, $Pca2_1$, $a = 27.829(3)$, $b = 10.3904(11)$, $c = 10.4664(11)$ Å, $Z = 4$, R_1 $[I > 2\sigma(I)] = 0.0387$, wR_2 $[I > 2\sigma(I)] = 0.0840$) were determined using single-crystal X-ray methods.

Keywords: Monobenzotetraazacyclo[15]annulenenickel(II); X-ray structure; Spectroscopy; Electrochemistry; Reactivity

1. Introduction

There are many reports of the reactivities of tetraazaannulene ligands and their transition metal complexes because of their potential as model compounds for porphyrins and corrins in biological systems. These include effects of the introduction of functional groups on the periphery of the macrocyclic ring [1–7]. However, most tetraazaannulene metal complexes prepared by the Jäger method are symmetric

*Corresponding author. Email: ychpark@mail.knu.ac.kr

Journal of Coordination Chemistry
ISSN 0095-8972 print/ISSN 1029-0389 online © 2007 Taylor & Francis
DOI: 10.1080/00958970600794875

complexes with 14-membered rings [8–10]. Corresponding 15-membered asymmetric tetraazaannulene complexes have rarely been investigated.

We have reported the synthesis, characterization and electrochemical properties of asymmetric tetraazaannulene nickel(II) complexes with 14- or 15-membered rings [11–15]. Here, we report of asymmetric monobenzotetraazaannulenenickel(II) complexes with two *p*-Xbenzoyl groups (X = CH_3, H, Cl, NO_2, OCH_3) in a 15-membered macrocycle. Electronic effects of substituents on spectroscopic properties (IR, ^1H, ^{13}C NMR, electronic absorption) and electrochemistry have been investigated. This provides some information about the reactivity of the methine sites in the ring. Such complexes have been used as catalysts in oxidation and reduction of substrates such as styrene or its derivatives and simple species such as O_2. This study is useful to summarize catalytic properties of tetraazaannulene complexes. The crystal structures of 2,4,10,12-tetramethyl-1,5,9,13-monobenzotetraazacyclo[15]annulenenickel(II) and 3,11-di(*p*-methylbenzoyl)-2,4,10,12-tetramethyl-1,5,9,13-monobenzotetraazacyclo[15]-annulenenickel(II) were determined using X-ray diffraction methods.

2. Experimental

2.1. *Materials and measurements*

$Ni(OAc)_2 \cdot 4H_2O$, 1,2-phenylenediamine, 1,3-diaminopropane, 2,4-pentandione and *p*-Xbenzoyl chloride (X = CH_3, H, Cl, NO_2 and OCH_3) were commercial chemicals. CH_3OH, CH_3CH_2OH and CH_2Cl_2 were refluxed over calcium hydride under nitrogen, and checked for their purity by GC before use. DMSO purchased from Merck was used without further purification. Tetraethylammoniumperchlorate (TEAP) was prepared and purified by a method described in the literature [6].

Elemental analyses (CHN) were carried out on a Carlo Erra, EA 1108 instrument. IR spectra (KBr pellets) were recorded on a Matteson Instruments Galaxy 7020 A spectrophotometer. ^1H and ^{13}C NMR spectra (300 MHz) were recorded on a Brucker instrument at room temperature and chemical shifts in $CDCl_3$ are given in ppm relative to tetramethylsilane as internal reference. Electronic absorption spectra were obtained using a Shimadzu UV-265 spectrophotometer. EI mass spectra were determined with a JEOL MS-DX 300 GC mass spectrometer at 70 eV using a direct inlet system. Cyclic voltammetry was performed using a Bioanalytical System (BAS) CV-50 W electrochemical analyzer and C2 cell stand at room temperature. The three-electrode system for the electrochemical measurements comprised a glassy carbon working electrode, an Ag/Ag^+ (0.01 M $AgNO_3$ in 0.1 M TEAP DMSO solution) reference electrode and a platinum wire auxiliary electrode.

2.2. *Synthesis of complexes*

The dark violet complex **1** was prepared in 30% yield by a method reported in the literature [11–13] (scheme 1). Anal. Calcd for $C_{19}H_{24}N_4Ni$ (%): C, 62.18; H, 6.54; N, 15.27. Found: C, 61.85; H, 6.72; N, 15.03. IR (cm^{-1}): ν(C=C), 1534; ν(C=N), 1551; $\nu(C_6H_6)$, 737. Electronic spectrum, $\lambda_{max}/nm(\varepsilon/M^{-1}\,cm^{-1})$, in chloroform: 379(26900), 574(2200). EIMS: m/z 366 $[M]^+$.

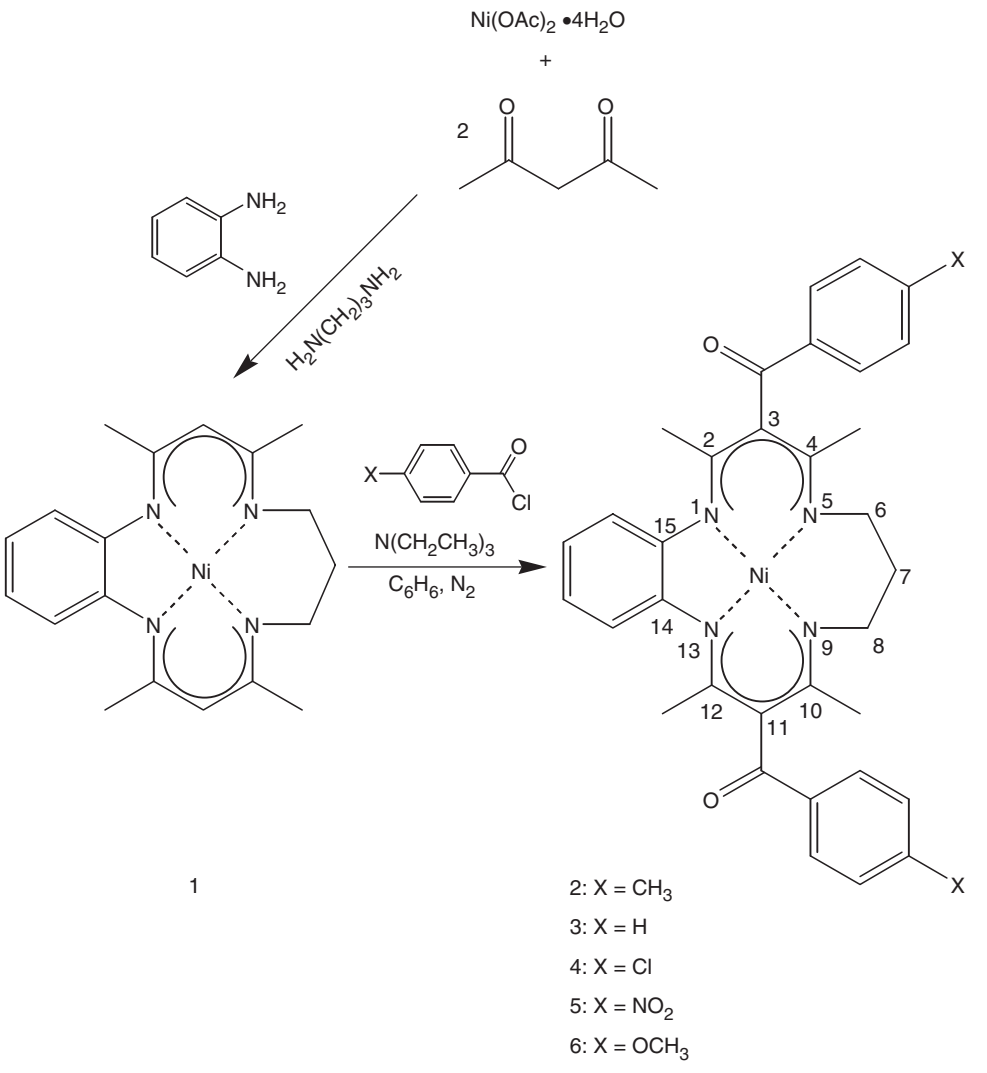

Scheme 1. Synthesis of asymmetric 15-membered dibenzoylmonobenzotetraazaannulenenickel(II) complexes.

2.2.1. 3,11-Di(*p*-methylbenzoyl)-2,4,10,12-tetramethyl-1,5,9,13-monobenzotetraazacyclo-[15]annulenenickel(II) (2). Complex **1** (0.366 g, 0.001 mol) was dissolved in benzene (50 cm^3) containing triethylamine (0.203 g, 0.002 mol) and *p*-Xbenzoyl chloride (0.002 mol) in benzene (30 cm^3) was added using a dropping funnel. The mixture was heated under reflux for 4 h with stirring and bubbling nitrogen gas to exclude moisture. The reaction mixture was then left to stand for 24 h at room temperature and filtered. The filtrate was evaporated to dryness under reduced pressure and the resulting solid was recrystallized from a 1 : 2 mixture of dichloromethane and methanol (or *n*-hexane) to obtain violet crystals. Yield: 0.18 g (30%). Anal. Calcd for $C_{35}H_{36}N_4O_2Ni$ (%): C, 69.67; H, 6.01; N, 9.28. Found: C, 69.51; H, 6.01; N, 9.11.

IR (cm^{-1}): ν(C=C), 1531; ν(C=N), 1604; ν(C=O), 1637; ν(aromatic), 749 and 847. Electronic spectrum, $\lambda_{max}/nm(\varepsilon/M^{-1}cm^{-1})$, in chloroform: 374(33000), 536(6000). EIMS: m/z 602 $[M]^+$.

2.2.2. 3,11-Di(*p*-Xbenzoyl)-2,4,10,12-tetramethyl-1,5,9,13-monobenzotetraazacyclo[15]-annulene nickel (II): X = H (3), Cl (4), NO_2 (5) and OCH_3 (6). The complexes **3**, **4**, **5**, and **6** were prepared by reaction of **1** (0.001 mol) with triethylamine (0.002 mol) and the corresponding *p*-Xbenzoyl chloride (0.002 mol) in benzene by modifying the processes described above. For **3**, yield = 0.28 g (48%). Anal. Calcd For $C_{33}H_{32}N_4O_2Ni$ (%): C, 68.89; H, 5.61; N, 9.74. Found: C, 68.85; H, 5.53; N, 9.70. IR (cm^{-1}): ν(C=C), 1530; ν(C=N), 1606; ν(C=O), 1632; ν(aromatic), 734 and 854. Electronic spectrum, $\lambda_{max}/nm(\varepsilon/M^{-1}cm^{-1})$, in chloroform: 374(27000), 531(5500). EIMS: m/z 574 $[M]^+$. For **4**, yield 0.33 g (51%). Anal. Calcd For $C_{33}H_{30}N_4O_2Cl_2Ni$ (%): C, 61.52; H, 4.69; N, 8.70. Found: C, 61.41; H, 4.53; N, 8.52. IR (cm^{-1}): ν(C=C), 1529; ν(C=N), 1584; ν(C=O), 1634; ν(aromatic), 751 and 850. Electronic spectrum, $\lambda_{max}/nm(\varepsilon/M^{-1}cm^{-1})$, in chloroform: 372(39000), 528(7500). EIMS: m/z 644 $[M]^+$. For **5**, yield 0.10 g (15%). Anal. Calcd For $C_{33}H_{30}N_6O_6Ni$ (%): C, 59.57; H, 4.54; N, 12.63. Found: C, 59.33; H, 4.44; N, 12.48. IR (cm^{-1}): ν(C=C), 1533; ν(C=N), 1598; ν(C=O), 1629; $\nu(NO_2)$, 1346; ν(aromatic), 739 and 852. Electronic spectrum, $\lambda_{max}/nm(\varepsilon/M^{-1}cm^{-1})$, in chloroform: 364(23000), 518(7500). EIMS: m/z 664 $[M]^+$. For **6**, yield 0.29 g (45%). Anal. Calcd for $C_{35}H_{36}N_4O_4Ni$ (%): C, 66.16; H, 5.71; N, 8.82. Found: C, 66.12; H, 5.54; N, 8.80. IR (cm^{-1}): ν(C=C), 1529; ν(C=N), 1597; ν(C=O), 1628; ν(aromatic), 748 and 846. Electronic spectrum, $\lambda_{max}/nm(\varepsilon/M^{-1}cm^{-1})$, in chloroform: 375(34500), 538(7000). EIMS: m/z 634 $[M]^+$.

2.3. *X-ray crystallography*

Preliminary examinations and data collection for crystals **1** and **2** were performed with Mo-Kα radiation ($\lambda = 0.71073$ Å) on an Enraf-Nonius CAD4 *k*-axis diffractometer equipped with a graphite crystal, incident-beam monochromator. Cell constants and orientation matrices for data collection were obtained from least-squares refinement using the setting angles of 25 reflections. Data were collected for Lorentz-polarization and absorption. The structures were solved by direct methods using SHELXS-86 [16] and refined by full-matrix least-squares calculations with SHELXL-97 [17]. The final cycle of the refinement converged with $R_1 = 0.0295$ and $wR_2 = 0.0744$ for **1** and $R_1 = 0.0387$ and $wR_2 = 0.0840$ for complex **2**.

3. Results and discussion

The asymmetric 15-membered dibenzoylmonobenzotetraazaannulenenickel(II) complexes were synthesized by following the synthetic procedure illustrated in scheme 1. Reaction of **1** with *p*-Xbenzoyl chloride in a 2 : 1 mole ratio was carried out in refluxing benzene in the presence of triethylamine and led to the corresponding di(*p*-Xbenzoyl)tetraaza[15]annulenenickel(II) complexes (**2**–**6**) in 15–51% yield. Elemental analyses and EI mass spectra were consistent with their formulae.

3.1. *Spectroscopic properties*

Characteristic IR data are given in the Experimental section. Spectra of complexes **2**–**6** showed an intense band due to C=O stretching of the benzoyl group at 1628–1637 cm^{-1} and bands due to C=C and C=N modes at 1529–1533 cm^{-1} and 1584–1606 cm^{-1}, respectively. Aromatic bands associated with the macrocycle and benzoyl group appeared at around 750 and 850 cm^{-1}, respectively. The substituent effect of benzoyl group on C=C, C=O and aromatic band energies were slight, but its influence on the C=N mode was clear. The effect of benzoylation is less for the 15-membered than for 14-membered complexes because of the difference in their ring strains. Complex **5** had a strong band at 1346 cm^{-1} associated with the NO_2 group.

Electronic absorption spectra of **1**–**6** showed two bands around 370 and 580 nm. The near-UV bands are attributed to $\pi \rightarrow \pi^*$ transitions. Spectra in the visible region showed bands between 510 and 540 nm ($\varepsilon_{max} = 2200$–$7500\ M^{-1}\,cm^{-1}$), attributed to ligand-to-metal charge transfer (LMCT) from the highest occupied ligand molecular orbital to the lowest empty d-orbital of nickel(II). The bands of **2**–**6** appear at higher energies (20–40 nm) than that of complex **1**. Variation of the electronic transition energies of the complexes with substituents (OCH_3, CH_3, H, Cl, NO_2) on the benzoyl groups was examined by a Hammett plot. As shown in figure 1, the energies of $\pi \rightarrow \pi^*$ and LMCT transitions against substituent parameters ($2\sigma_p$) of the benzoyl groups were

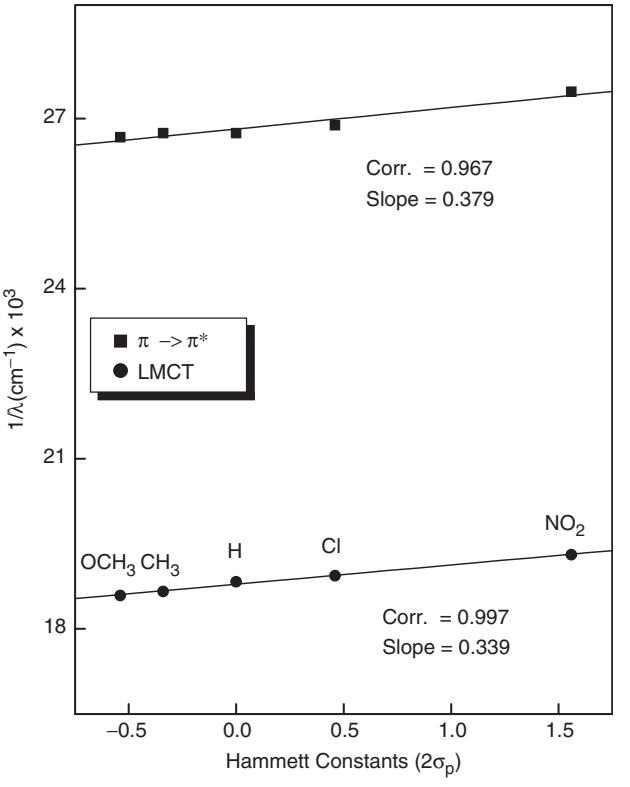

Figure 1. Correlation between the maximum energies ($1/\lambda_{max}$) of the $\pi \rightarrow \pi^*$ and LMCT of complexes **2**–**6** and Hammett constants ($2\sigma_p$).

Table 1. ^{1}H-NMR data for complexes **1**–**6**.[a]

No.	Methyl	Methine	Propylene	X	Aromatic (macrocycle)	Aromatic (benzoyl)
1	2.082(s)	4.876(s)	2.313(s)		6.634–6.832(m)	
	2.373(s)		2.815(s)			
2	1.758(s)		2.716(s)	2.447(s)	6.735–6.791(m)	7.288(d)
	2.160(s)		2.885(s)			7.902(d)
3	1.756(s)		2.736(s)		6.767–6.803(m)	7.497 ~ 8.002(m)
	2.199(s)		2.896(s)			
4	1.746(s)		2.745(s)		6.780(br)	7.453(d)
	2.188(s)		2.891(s)			7.913(d)
5	1.743(s)		2.883(s)		6.811(br)	8.070(d)
	2.251(s)		2.911(s)			8.327(d)
6	1.773(s)		2.697(s)	3.896(s)	6.734–6.786(m)	6.974(d)
	2.123(s)		2.887(s)			7.993(d)

[a] Chemical shifts in ppm from TMS as internal reference; measured in $CDCl_3$ at 300 MHz; multiplicity of a proton signal is given in parentheses after the δ value; s = singlet, d = doublet, br = broad, m = multiplet.

linear with positive slopes +0.379 for $\pi \rightarrow \pi^*$ and +0.339 for LMCT. Such effects on electronic transition energies for the 15-membered complexes are less than those for 14-membered tetraazaannulenenickel(II) analogues (slope +0.224 for $\pi \rightarrow \pi^*$ and −0.250 for LMCT) [18]. This may be due to a more distorted square planar structure for the 15-membered tetraazaannulene complexes than for the 14-membered complexes. The π conjugation system could not be extended by benzoylation.

Proton NMR data for the complexes are colleted in table 1. The methine signal of **1** appeared at 4.876 ppm (4.88 ppm [12]), but in complexes **2**–**6** disappeared due to benzoylation. Peaks due to 4,10- and 2,12-methyl protons of the complexes are shifted upfield by about 0.3 and 0.2 ppm, respectively, compared to those of complex **1**, due to anisotropic effects of the benzoyl group. Other proton signals (propylene and benzene) on the macrocycle moved downfield owing to deshielding effects of the benzoyl group. This indicates that the benzoyl groups are not perpendicular to the macrocycle ring plane and affect the NMR resonances of the 4,10-methyl more than the 2,12-methyl protons.

^{13}C NMR data and assignments for the complexes are listed in table 2. Carbon peaks of the complexes shifted downfield due to deshielding in a different way to the proton spectra. New carbon signals for the carbonyl and phenyl group upon benzoylation were observed at 195–2199 and 114–164 ppm, respectively. The methine signals were the most affected, moving downfield by about 14 ppm owing to the electron-withdrawing character of the benzoyl group.

3.2. *Electrochemical behaviour and Hammett plots*

Redox potentials of the asymmetric complexes before and after dibenzoylation were measured in 0.1 M TEAP-DMSO solutions *vs* Ag/Ag^+ (0.01 M) at 25°C and sweep rates of 100 mV s^{-1}; data are listed in table 3. Voltammograms of **2**–**6** showed two irreversible oxidation potentials which are ligand-centred (Mc) in the range +0.440 to +0.850 V ($Mc/Mc^{\bullet +}$ and $Mc^{\bullet +}/Mc^{2+}$). A quasi-reversible reduction peak ($Ni^{2+} \rightarrow Ni^{+}$) appeared in the range −2.550 to −2.690 V. The first two peaks must be associated with the benzoyl group and their substituents because complex **1** had only one reduction peak. The oxidation of the tetraazaannulene ring shifted toward positive values according

Table 2. ^{13}C-NMR data for complexes **1**–**6**.[a]

No.	Methyl	Methine	Propylene	X	Aromatic (macrocycle)	Aromatic (benzoyl)	C=N	C=O
1	21.035	103.972	50.904		120.051		155.012	
	21.258		31.887		120.451		160.462	
					146.096			
2	21.150	117.949	52.194	21.554	121.638	129.242	158.639	197.906
	21.554		32.297		121.751	129.517	162.911	
					139.823	142.574		
						146.408		
3	21.649	118.509	51.597		122.285	128.945	159.797	198.193
	22.295		32.661		122.609	129.745	163.928	
					133.173	143.026		
						146.780		
4	21.781	118.200	51.626		122.303	129.238	160.104	196.716
	22.420		32.632		122.507	131.081	163.912	
					138.568	141.431		
						146.657		
5	22.076	118.747	51.994		123.141	120.622	160.550	195.586
	23.258		31.842		123.631	129.869	163.266	
					145.018	148.977		
						149.528		
6	21.530	117.995	51.659	55.854	121.950	114.132	158.412	197.782
	21.770		32.757		122.137	132.058	162.778	
					146.782	135.346		
						163.281		

[a] Chemical shifts in ppm from internal TMS; measured in chloroform-d at room temperature.

Table 3. Redox potential data for complexes **1**–**6**.[a]

Comp.	$E_{op(1)}$, mV $0 \rightarrow +1$	$E_{op(2)}$, mV $+1 \rightarrow +2$	$E_{rp(1)}$, mV $0 \rightarrow -1$	$E_{rp(2)}$, mV $-1 \rightarrow -2$	$E_{rp(m)}$, mV $Ni^{2+} \rightarrow Ni^{+}$
1	+131	+604			−2426
2	+372	+775	−2255	−2419	−2590
3	+378	+777	−2237		−2533
4	+399	+810	−2124	−2329	−2533
5	+433	+854	−1263	−1798	−2694
6	+356	+748	−2250	−2511	−2672

[a] All data were measured in 0.1 M TEAP-DMSO solutions *vs.* Ag/Ag^{+} (0.01 M $AgNO_3$ in DMSO) at 25°C.

to the electron-withdrawing substituents on the benzoyl group, while the reduction potentials ($Ni^{2+} \rightarrow Ni^{+}$) were only slightly affected. Oxidation potentials were in the order $NO_2 > Cl > H > CH_3 > OCH_3$ and substituent effects were examined by means of a Hammett plot. As shown in figure 2, the relationships between the first and second oxidation potentials and $2\sigma_p$ were linear with slopes of +0.071 and +0.104, respectively.

3.3. *X-ray structures of 1 and 2*

The crystal structures of 2,4,10,12-tetramethyl-1,5,9,13-monobenzotetraazacyclo-[15]annulenenickel(II) and 3,11-di(*p*-methylbenzoyl)-2,4,10,12-tetramethyl-1,5,9,13-monobenzotetraazacyclo[15]annulenenickel(II) are illustrated in figures 3

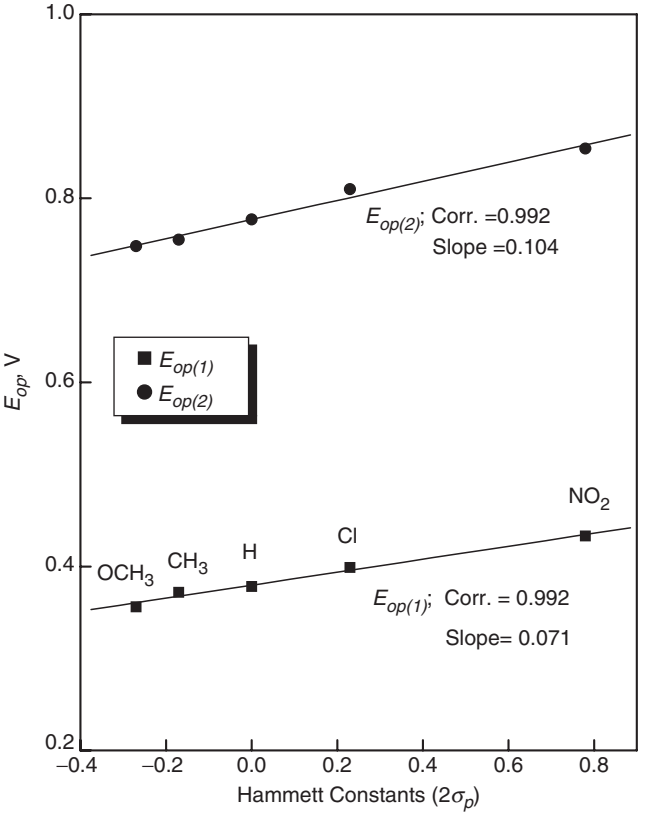

Figure 2. Hammett plots of 1st and 2nd oxidation potentials *vs.* 2σp for complexes 2–6.

and 4, respectively. Crystal data and refinement parameters are listed in table 4 and selected bond distances and angles in table 5. Average of Ni(1)–N(1) and Ni(1)–N(2) bond lengths (1.8830 Å for **1** and 1.8755 Å for **2**) are somewhat shorter than those of Ni(1)–N(3) and Ni(1)–N(4) (1.9072 Å for **1** and 1.894 Å for **2**), while in the asymmetric tetraaazacyclo[14]annulenenickel(II) complex the Ni–N(phenylenediamine) are somewhat longer than Ni–N(ethylenediamine) bond distances owing to the higher basicity of ethylenediamine. Although the basicity of phenylenediamine is smaller than that of propylenediamine, in **1** and **2** the Ni(1)–N(1) and Ni(1)–N(2) distances are shorter than Ni(1)–N(3) and Ni(1)–N(4). This may be due to the different ring sizes. N–Ni–N angles of five membered rings in **1** and **2** are 83.13 and 84.43°, respectively, smaller than in the 14-membered tetraazacyclo[14]annulenenickel(II) complex (about 86° [18, 19]) owing to the longer chain length of propylenediamine. Average of N(1)–Ni–N(3) and N(2)–Ni–N(4) angles for **1** and **2** are 173.8 and 174.25°, respectively. These results indicate that the Ni(II) atom coordinated by four nitrogen atoms exhibits some square pyramidal distotion due to the ring strain of propylenediamine. In addition, the macrocycle ring is little affected by the benzoyl groups after benzoylation.

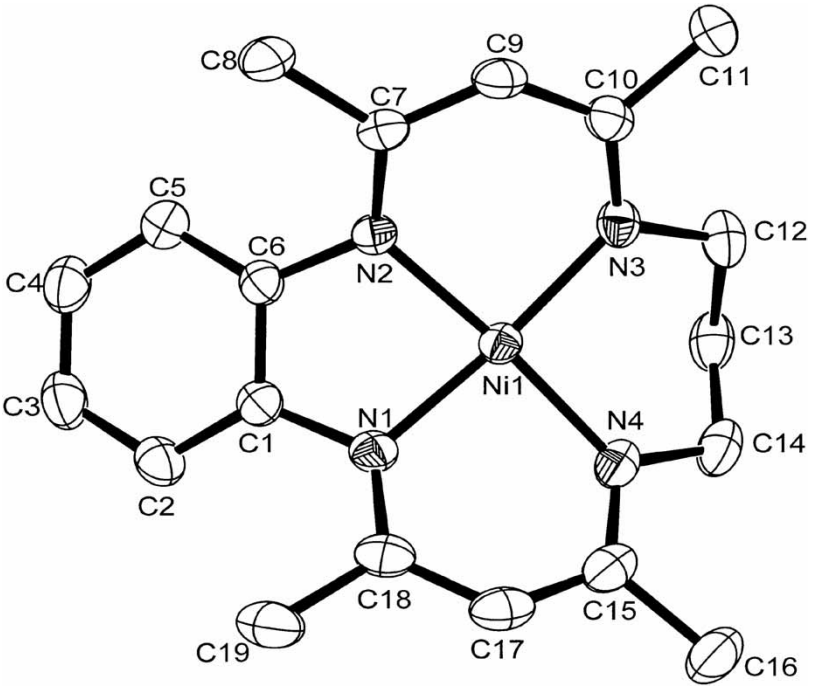

Figure 3. The molecular structure of complex **1** showing the atom numbering scheme.

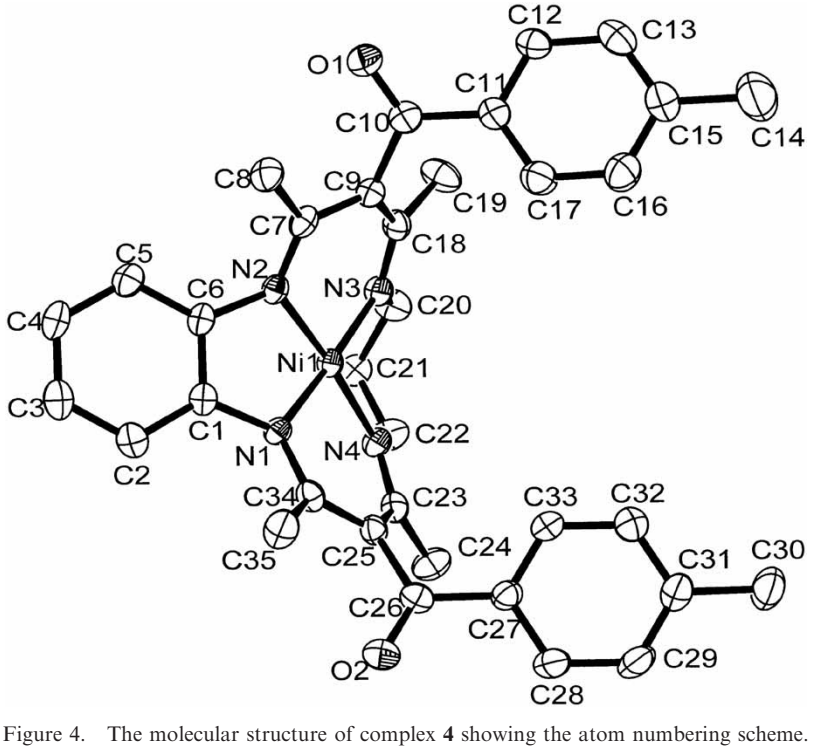

Figure 4. The molecular structure of complex **4** showing the atom numbering scheme.

Table 4. Crystal data and structure refinement details for **1** and **2**.

Empirical formula	$C_{19}H_{24}N_4Ni$	$C_{35}H_{36}N_4O_2Ni$
Formula weight	367.13	603.39
Temperature (K)	173(2)	173(2)
Wavelength (Å)	0.71069	0.71073
Crystal system	Monoclinic	Orthorhombic
Space group	$C2/c$	$Pca2_1$
Unit cell dimensions (Å, °)		
a	22.883(6)	27.829(3)
b	10.358(3)	10.3904(11)
c	14.755(4)	10.4664(11)
β	102.704(4)	
V (Å^3)	3411.6(14)	3026.4(6)
Z	8	4
Density (calculated) (Mg m^{-3})	1.430	1.324
Absorption coefficient (mm^{-1})	1.145	1.679
$F(000)$	1552	1272
Crystal size (mm^3)	$0.45 \times 0.40 \times 0.13$	$0.50 \times 0.28 \times 0.10$
Theta range for data collection (°)	1.82–28.32	1.96–28.30
Index ranges	$-30 \le h \le 19$	$-33 \le h \le 36$
	$-12 \le k \le 13$	$-10 \le k \le 13$
	$-19 \le l \le 19$	$-12 \le l \le 13$
Reflections collected	10267	18092
Independent reflections	4046 [R(int) = 0.0199]	7127 [R(int) = 0.0319]
Completeness to theta	95.2% (28.32°)	98.0% (28.30°)
Absorption correction	Semi-empirical from equivalents	Semi-empirical from equivalents
Max. and min. transmission	0.8654 and 0.6269	0.9352 and 0.7276
Refinement method	Full-matrix least-squares on F^2	Full-matrix least-squares on F^2
Data/restraints/parameters	4046/0/313	7126/1/385
Goodness-of-fit on F^2	1.019	1.01
Final R indices [$I > 2\sigma(I)$]	$R_1 = 0.0295$, $wR_2 = 0.0744$	$R_1 = 0.0387$, $wR_2 = 0.0840$
R indices (all data)	$R_1 = 0.0367$, $wR_2 = 0.0793$	$R_1 = 0.0565$, $wR_2 = 0.0915$
Largest diff. peak and hole (e Å^{-3})	0.668 and −0.228	0.693 and −0.295

Table 5. Selected bond distances (Å) and angles (°) for **1** and **2**.

	1	**2**
N(1)–Ni(1)	1.8868(15)	1.877(2)
N(2)–Ni(1)	1.8791(13)	1.874(2)
N(3)–Ni(1)	1.9144(15)	1.888(2)
N(4)–Ni(1)	1.9100(14)	1.900(2)
N(1)–Ni(1)–N(3)	173.01(6)	174.53(9)
N(2)–Ni(1)–N(4)	174.59(6)	173.97(10)
N(1)–Ni(1)–N(2)	83.13(6)	84.43(9)
N(1)–Ni(1)–N(4)	91.55(6)	89.71(9)
N(2)–Ni(1)–N(3)	91.21(6)	90.40(9)
N(3)–Ni(1)–N(4)	94.01(6)	95.50(9)

Supplementary material

Crystallographic data for the structures have been deposited at the CCDC, 12 Union Road, Cambridge CB2 1EZ, UK, and are available on request, quoting deposition numbers CCDC 245072 (**1**) and CCDC 245073 (**2**). Copies of the information can be obtained free of charge via E-mail: deposit@ccdc.cam.ac.uk or www: http://www.ccdc.cam.ac.uk; Tel: +44-1233-336031; Fax: +44-1223-336033.

Acknowledgement

This work was supported by a Korea Research Foundation Grant (KRF-2006-005-C00009).

References

[1] D.A. Place, G.P. Ferrara, J.J. Harland, J.C. Dabrowiak. *J. Heterocyclic Chem.*, **17**, 439 (1980).
[2] C.L. Bailey, R.D. Bereman, D.P. Rillema. *Inorg. Chem.*, **25**, 3149 (1986).
[3] J.C. Dabrowiak, D.P. Fisher, F.C. McElroy, D.J. Macero. *Inorg. Chem.*, **18**, 2304 (1979).
[4] J. Eilmes, O. Michalski, K. Woźniak. *Inorg. Chim. Acta*, **317**, 103 (2001).
[5] K. Sakata, K. Koyanagi, M. Hashimoto. *J. Heterocyclic Chem.*, **32**, 329 (1995).
[6] P.J. Hochgesang, R.D. Bereman. *Inorg. Chim. Acta*, **156**, 213 (1989).
[7] E.M. Opozda, W. Lasocha. *Inorg. Chem. Commun.*, **3**, 239 (2000).
[8] C.L. Bailey, R.D. Bereman, D.P. Rillema, R. Nowak. *Inorg. Chem.*, **23**, 3956 (1984).
[9] K. Sakata, H. Tagami, M.J. Hashimoto. *J. Hetetrocyclic Chem.*, **26**, 805 (1989).
[10] K. Sakata, M. Hashimoto, T. Hamada, S. Matsuno. *Polyhedron*, **15**, 967 (1996).
[11] Y.C. Park, S.S. Kim, D.C. Lee, C.H. An. *Polyhedron*, **16**, 253 (1997).
[12] Y.C. Park, Z.U. Bae, S.S. Kim, S.K. Baek. *Bull. Korean Chem. Soc.*, **16**, 287 (1995).
[13] Y.C. Park, J.C. Byun, J.H. Choi, J.W. Lim, D.C. Lee, H.G. Na. *Polyhedron*, **21**, 917 (2002).
[14] Y.C. Park, S.S. Kim, Y.I. Noh, H.G. Na. *J. Coord. Chem.*, **41**, 191 (1997).
[15] Y.C. Park, H.G. Na, J.H. Choi, J.C. Byun, E.H. Kim, D.I. Kim. *J. Coord. Chem.*, **55**, 505 (2002).
[16] G.M. Sheldrick. *Acta Crystallogr.*, **A46**, 467 (1990).
[17] G.M. Sheldrick. *SHELX-97*, University of Göttingen, Germany (1997).
[18] Y.C. Park, J.H. Choi, H.G. Na, S.H. Shin, E.H. Kim, D.I. Kim. *J. Coord. Chem.*, **57**, 133 (2004).
[19] Y.C. Park, Z.U. Bae, H.G. Na, T.G. Roy, E.H. Kim, D.I. Kim. *J. Coord. Chem.*, **58**, 231 (2005).